Science Advances
AAAS

advances.sciencemag.org/cgi/content/full/4/10/eaau4029/DC1

# Supplementary Materials for

## The demise of Angkor: Systemic vulnerability of urban infrastructure to climatic variations

Dan Penny*, Cameron Zachreson, Roland Fletcher, David Lau, Joseph T. Lizier, Nicholas Fischer, Damian Evans, Christophe Pottier, Mikhail Prokopenko

*Corresponding author. Email: dan.penny@sydney.edu.au

Published 17 October 2018, *Sci. Adv.* **4**, eaau4029 (2018)
DOI: 10.1126/sciadv.aau4029

**This PDF file includes:**

**Supplementary Text**

Model details

Our model describes the topological evolution of an historic water distribution network. It does this by simulating the effects of fluid velocity on channel erosion and sedimentation. This model is phenomenological in that it does not explicitly simulate mass flow during erosion and re-deposition. Instead, it uses simple equations to describe a well-constrained dynamic within a minimal parameter space. Symbols for control and non-control parameters are given in tables S1 and S2, respectively. The main components of this model are as follows:

- topology: the network is assumed to be a directed, acyclic graph with a single source (or super source, **S**), and sink (or super sink **T**) (fig. S2). The edges represent undisrupted water channels, while the nodes represent locations at which channels meet.
- edge characteristics: An edge $e_{ij}$ between nodes $i$ and $j$ is defined by the fluid flow through it $(f_{ij})$, and its flow capacity $c_{ij}$ that approximates its cross-sectional area. We estimate the fluid velocity along an edge as the ratio of flow to capacity $v_{ij} = \frac{f_{ij}}{c_{ij}}$
- flow distribution: fluid flow is distributed from source to sink based on proportional splitting at nodes. Each edge exiting a node is apportioned flow based on its capacity relative to the capacities of the other edges exiting the same node. For example, if an input flow $f_i$ is split between edges $e_{ij}$ and $e_{ik}$ exiting the same node i with capacities $c_{ij} = 9$, and $c_{jk} = 1$, then $f_{ij} = 0.9f_i$ and $f_{jk} = 0.1f_i$
- erosion: edge capacities can change depending on fluid velocity. Erosion occurs if fluid velocity exceeds a threshold: $v_{max} = v_o/\alpha$, where $v_o$ is the fluid velocity at initialization, and $\alpha$ is a control parameter $\alpha\epsilon(0,1)$. If erosion occurs, capacity increases.
- sedimentation: sedimentation decreases edge capacity if flow velocity falls below a defined threshold $v_{min} = \beta v_o, \beta\epsilon(0,1)$ where $\beta$ is a free control parameter.
- perturbation: we model perturbations to the initial flow distribution as stochastic flooding. That is, random increases in flow applied to each edge, and an increase in the flow input at the source. These local perturbations are gamma-distributed, with shape parameter $\kappa$ and scale parameter $\theta_{ij} = f_{ij}^{o}\gamma/\kappa$, where $\kappa$ and $\gamma$ are control parameters defining the flood anisotropy and magnitude, respectively, and $f_{ij}^{o}$ is the flow on $e_{ij}$ at initialisation.

Initialization

The network is initialized as a valued, directed, acyclic graph. If multiple sinks or sources exist, the super source and sink **S** and **T** are added (fig. S2). The graph is initialized with some pre-specified edge weights $w_{ij}$. These edge weights are translated to initial capacities by distributing unit flow throughout the network, as described above but replacing $c_{ij}$ with $w_{ij}$ when apportioning the initial flows. We then normalize all flows to the smallest flow on any edge so that $f_{ij}^{o} \geq 1$. This produces the unperturbed network, prior to any disturbance. These initial flows are then assigned as capacities, so that on all edges the initial flow is equal to its capacity, and $v_o = 1$.

Perturbation

After initialization, each edge is randomly assigned a perturbation from a gamma distribution with shape parameter $\kappa$ and scale parameter $\gamma f_{ij}^{o}/\kappa$, where $\kappa$ and $\gamma$ are free parameters, both greater than zero. Additionally, the flow input to the (super) source is increased by a factor of gamma.

After adding the perturbations to the initial flows, the flow on each edge is resolved using the flow distribution rule discussed above. Once the flow at the (super) sink is equal to the total flow input (including all perturbations), flow velocities are re-calculated and if they meet the requirements for sedimentation or erosion, new capacities are established as follows

$$c_{ij}(t') = \begin{cases} c_{ij}(t) + \alpha f_{ij}\left[\dfrac{v_{ij}}{v_{max}}\right], & \text{if } v_{ij} > v_{max} \\ c_{ij}(t) - \beta f_{ij}\left[\dfrac{v_{min}}{v_{ij}}\right], & \text{if } v_{ij} < v_{min} \end{cases}$$

Equation 2

where $t'$ represents the next iteration of the algorithm and $t$ the current iteration. These equations for sedimentation and erosion reflect our assumptions that the rates of sedimentation or erosion depend on the flow magnitude (a small amount of fast-moving water removes proportionally less material than a large amount), and that the erosion or sedimentation rate per unit flow depends on the degree to which the fluid velocity has exceeded (or fallen short of) the threshold for that process. The coefficients $\alpha$ and $\beta$ express the tendency for erosion or sedimentation to occur.

Topological evolution

Because erosion or sedimentation on an edge changes the distribution of flow to the competing edges leaving the same node, local damage can produce feedback that changes the overall flow distribution in the network. This redistribution process converges as capacities change in response to altered flow velocities.

To decide if the network has reached a condition in which the perturbed flow distribution has stabilised, we calculate a damage metric $Q$ that reflects the re-distribution of flow within the network. This value measures both flow depletion as well as flooding by taking the ratio of the measured difference in flow to the maximum possible difference in either the negative or positive direction. To calculate this value, we distribute the original pre-flood flow into the damaged network with modified edge capacities, and compare the resulting flows to the initial ones

$$Q_{ij}(t) = \begin{cases} \dfrac{f_{ij} - f_{ij}^o}{f_{eq} - f_{ij}^o}, & \text{if } f_{ij} > f_{ij}^o \\ \dfrac{f_{ij}^o - f_{ij}}{f_{ij}^o}, & \text{if } f_{ij} \leq f_{ij}^o \end{cases}$$

Equation 3

where $f_{ij}$ is the flow on the damaged graph, $f_{ij}^o$ is the initial flow on edge $ij$ and $f_{eq}$ is the total flow input at equilibrium. We then calculate the damage value for the whole network by taking the average over all edges weighted to the initial flows

$$Q(t) = \frac{\Sigma_i \Sigma_j Q_{ij} f_{ij}^o}{\Sigma_i \Sigma_j f_{ij}^o}$$

Equation 4

To test whether the network damage has converged over the iteration $t \rightarrow t'$ we compute $\Delta Q = |Q(t') - Q(t)|/Q(t)$. If $\Delta Q$ is greater than a pre-defined convergence threshold $\Delta Q_{min}$, the flood scenario is repeated with a further iteration of the flow distribution algorithm, followed by updating capacities according to equation 3. When $\Delta Q$ has fallen below $\Delta Q_{min}$, we assign the convergence time $t_f(\alpha, \beta, \gamma, \kappa, \Delta Q_{min}) = t$ and the damage as a function of the control parameters: $\mathbf{Q}(\alpha, \beta, \gamma, \kappa) = Q(t_f)$. Note well that, in general, italicized Q ($Q$) is used in reference to local or time dependent damage while bold Q (**Q**) is used in reference to the whole network after time convergence.

Diamond network results

Generic diamond-shaped networks are shown in figures S3-S5. Plots of the average value of **Q** as a function of $\alpha$ and $\beta$ for two different values of $\gamma$ are shown in fig. S6. These plots demonstrate that the behaviour of the model discussed in main text is not limited to the specific topology of Angkor. The exact positions of the transitions between regions (i), (ii), and (iii), and the average damage for each combination of parameters, will depend on the network studied. However, the qualitative functional dependence of **Q** on the control parameters is conserved.

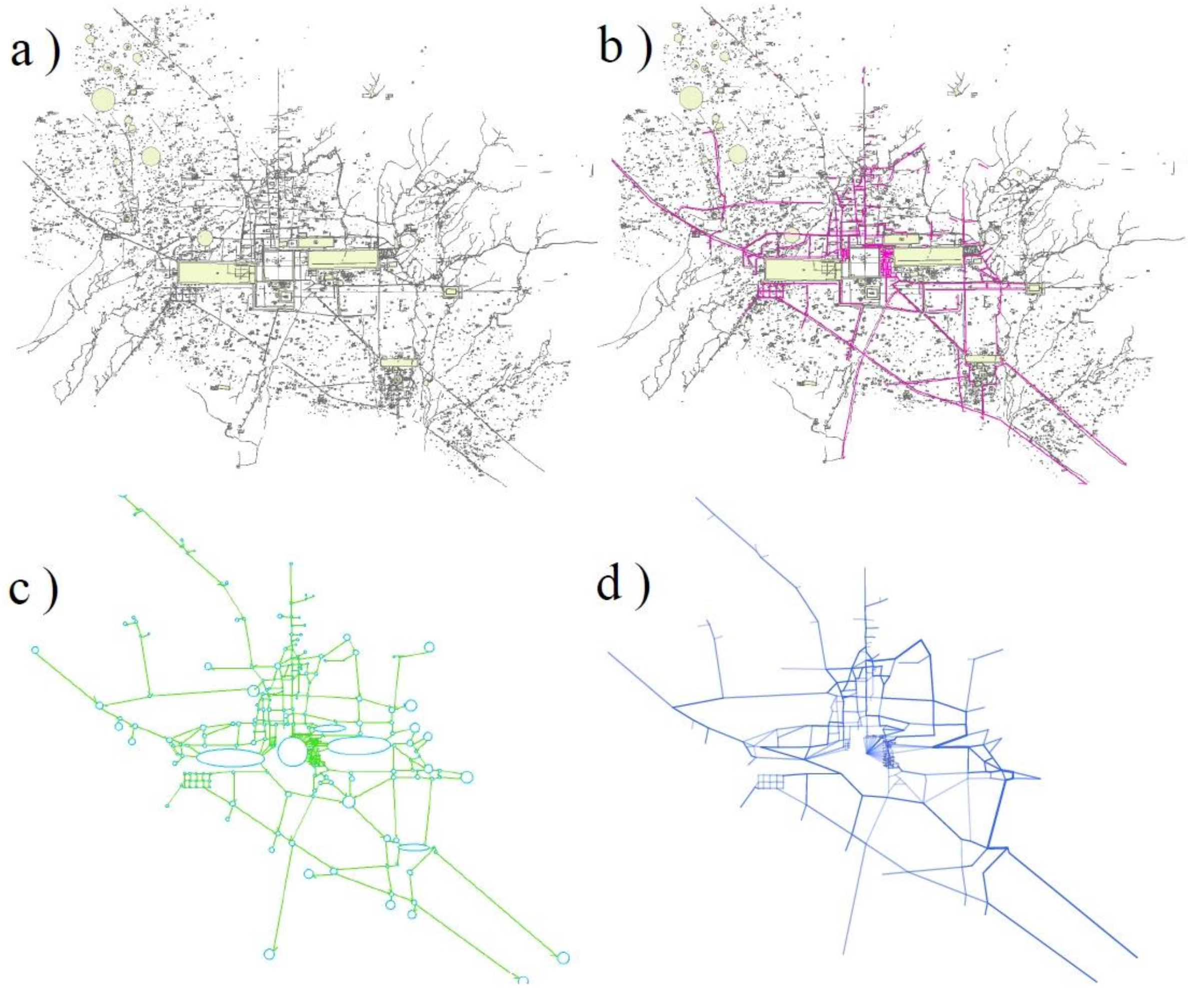


**Fig. S1. Conversion of archeological maps of 14th century Angkor into a directed, acyclic network topology.** We used the GIS maps originally created by *26, 30, 47, 46* (A), to delineate features of the irrigation system (B). We then translated these features into a network topology (C) by placing nodes (blue circles) at their intersections, and edges (green arrows) along their lengths. We assigned each edge one of three weights (1, 0.1, or 0.01) based on a rough estimation of its width, and a direction based on the topographical differential between its source and target nodes. Finally, starting from the source, we solved for the equilibrium flow on each edge by apportioning it based on the relative weights of the edges exiting each node (D).

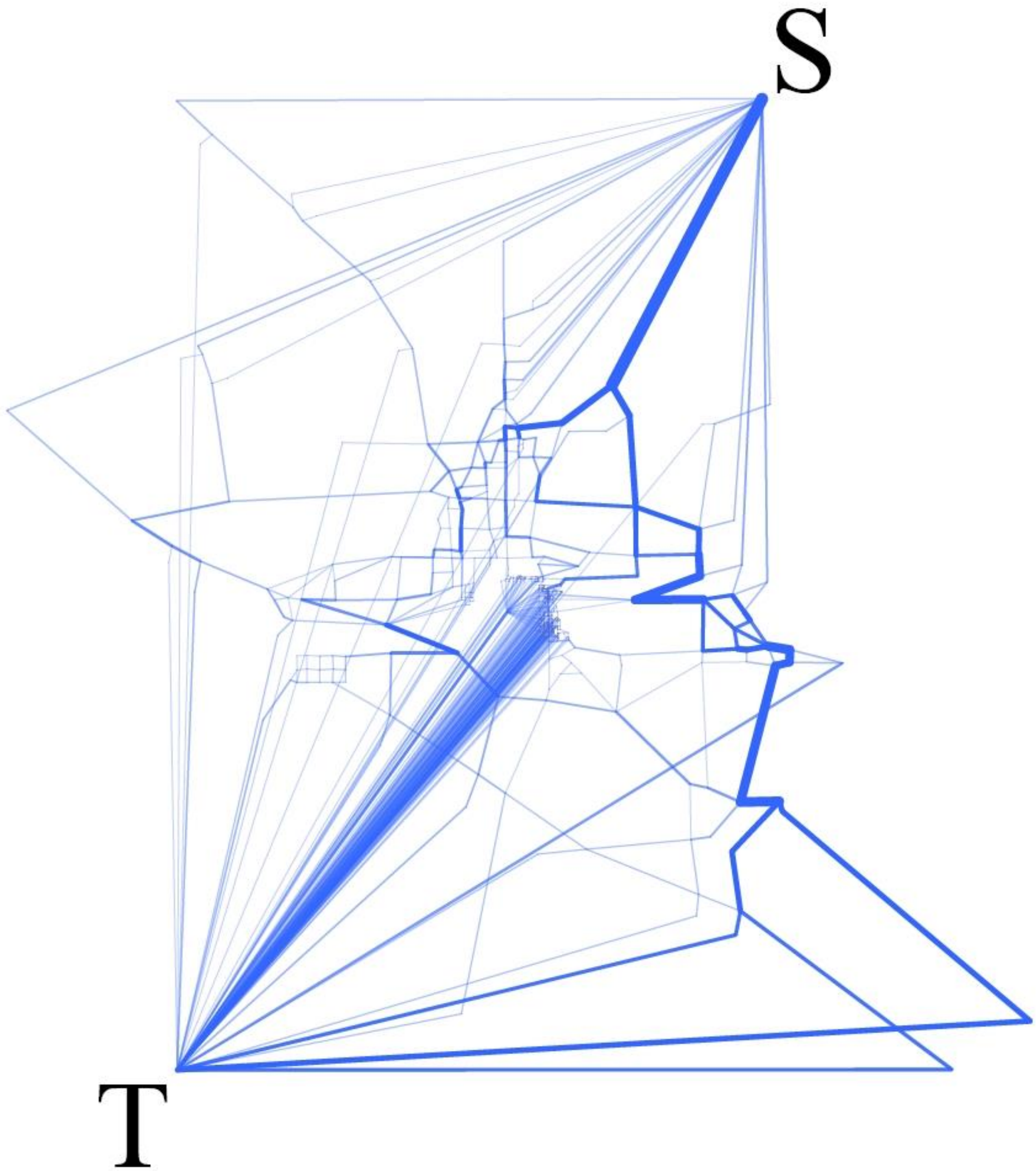


**Fig. S2. A map representing the Angkor network with supersource (S) and supersink (T) included.**

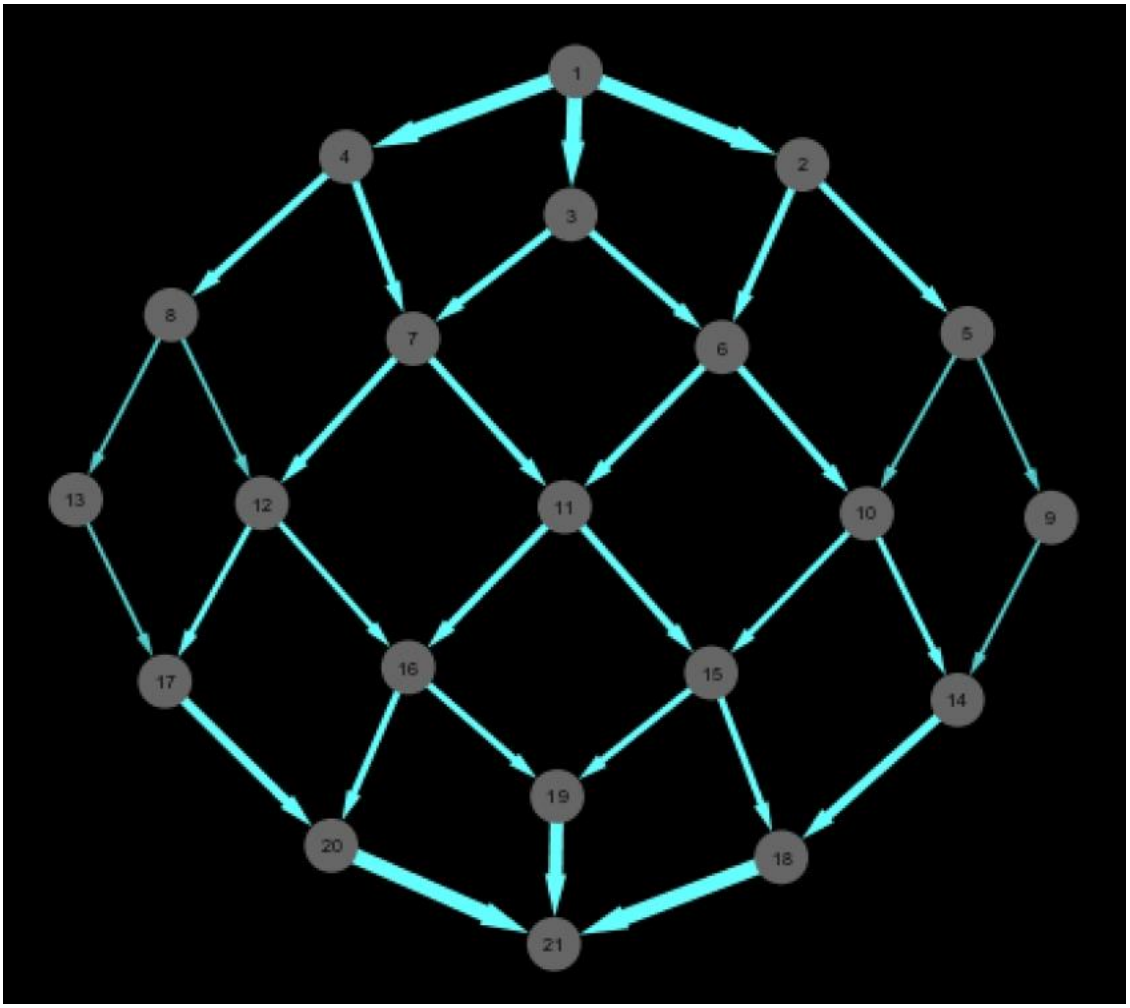


**Fig. S3. A generic network showing equilibrium flow distribution at initialization.** The width of each arrow is proportional to the flow ($f_{ij}^{o}$) on the corresponding edge.

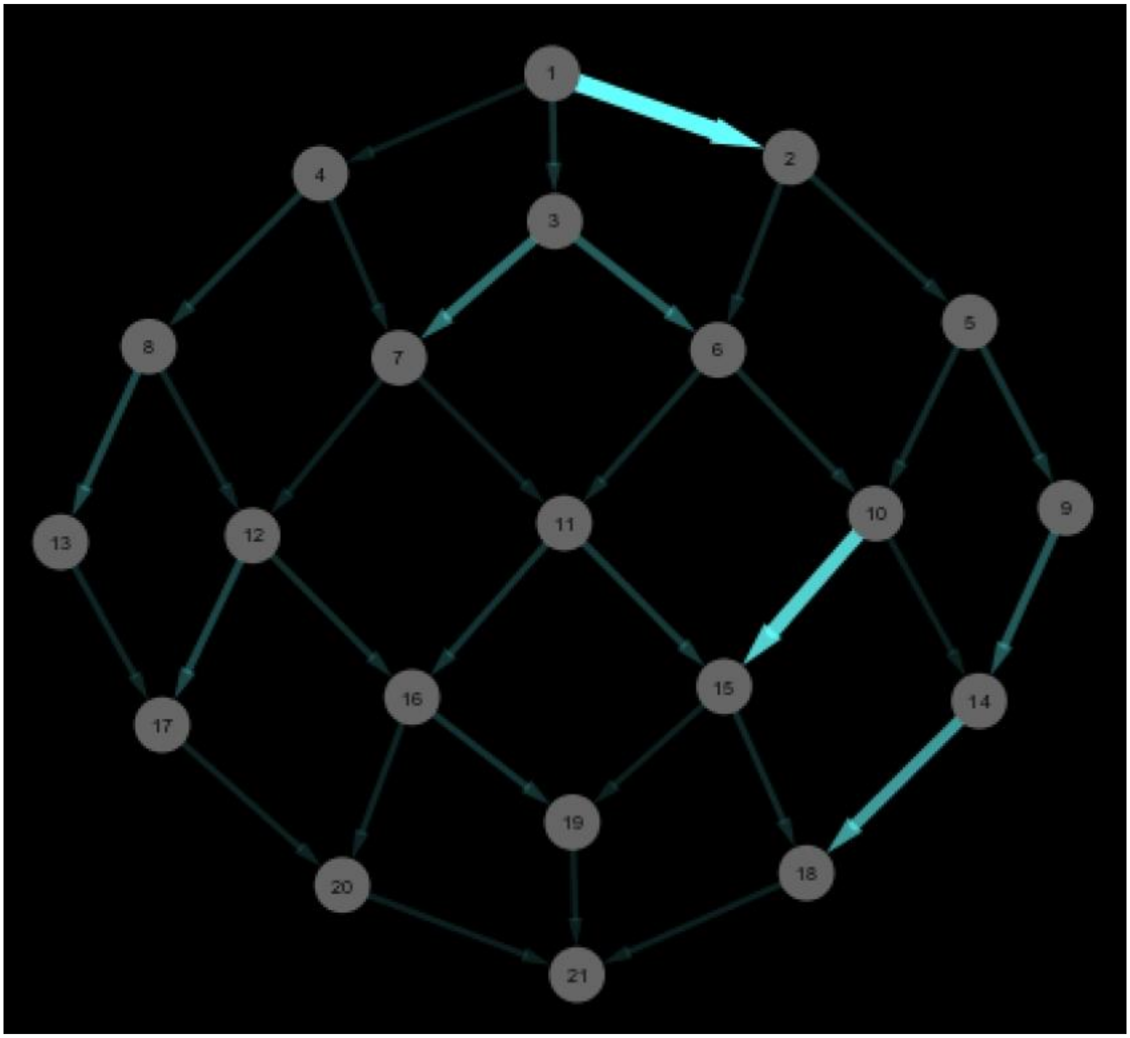


**Fig. S4. To induce damage, random flood flows are added to each edge.** Here, the perturbation is highly aniosotropic (the flood parameters are: $\kappa = 0.5$ and $\gamma = 1$).

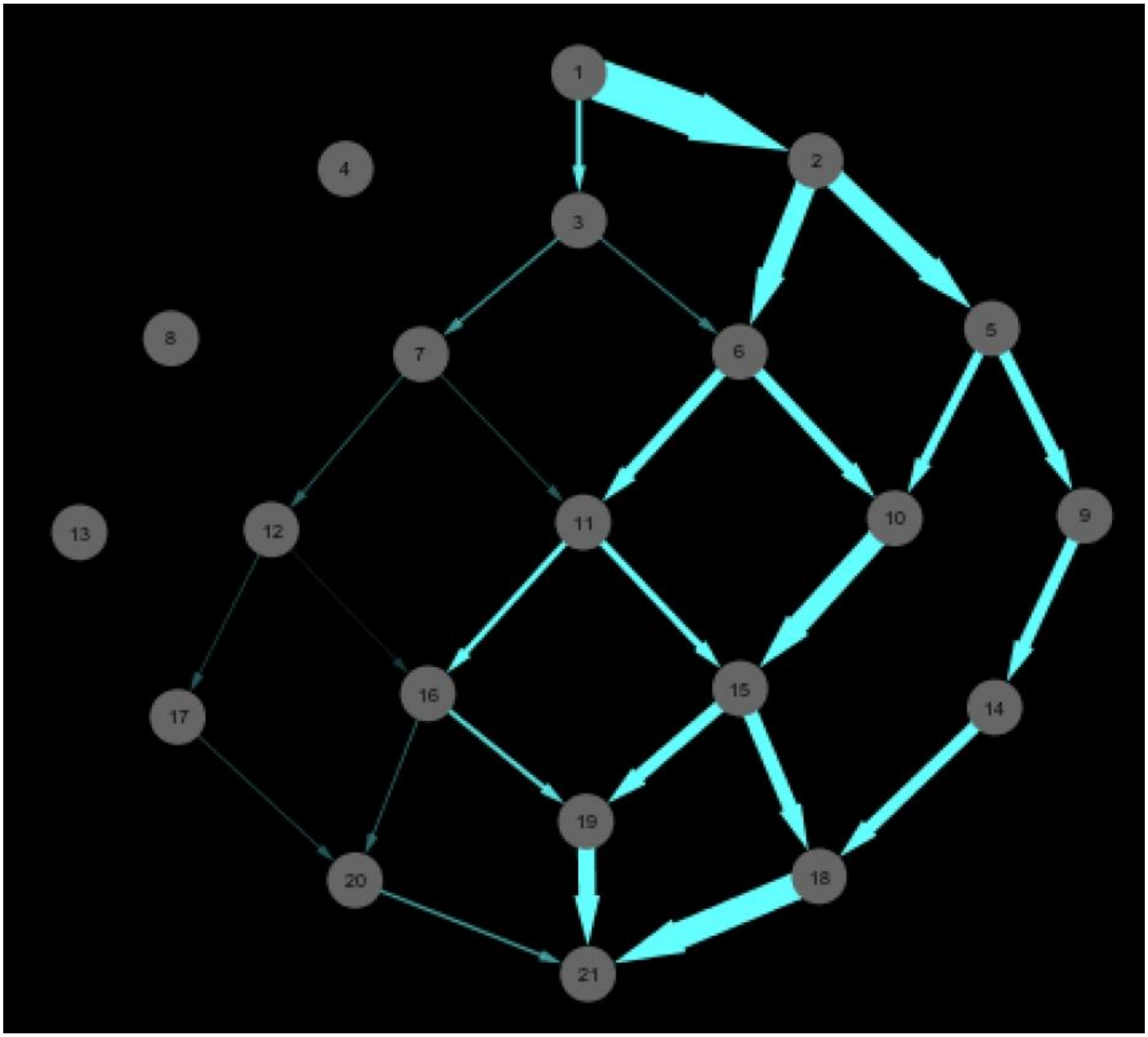


**Fig. S5. Final flow distribution resulting from the perturbation shown above, for $\alpha = 0.9$, $\beta = 0.9$, and $\Delta Q_{min} = 2 \times 10^{-3}$.**

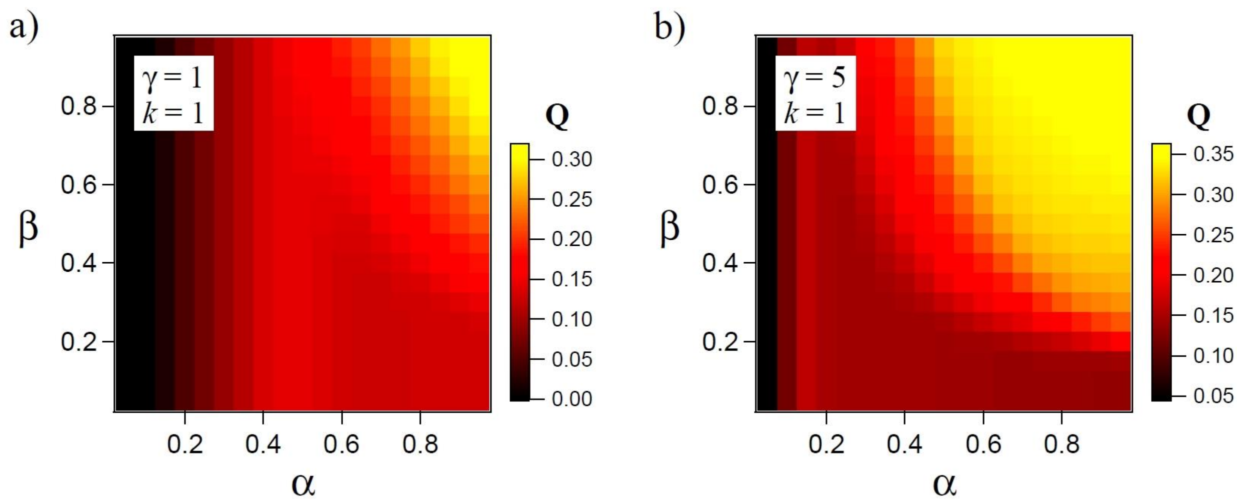


**Fig. S6. Results of the model on a generic topology.** Two-dimensional colour plots representing the behaviour of Q as a function of α and β for $\gamma = 1$ (a) and $\gamma = 5$ (b), for simulations on the 21-node diamond network discussed in the text. Each pixel represents an average over $n = 100$ different random flood configurations.

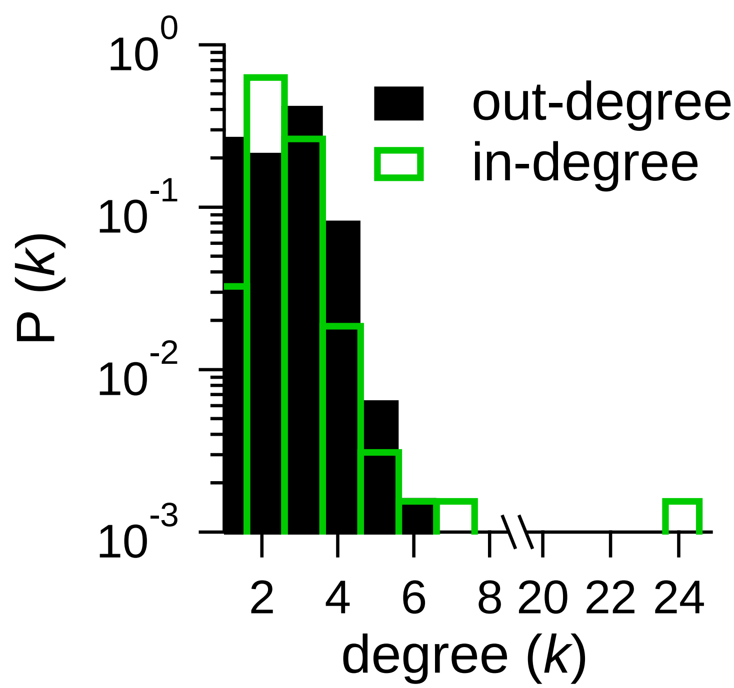


**Fig. S7. Probability distribution for indegree and outdegree of each node in the final network representation of Angkor's water distribution network, with supersource and supersink omitted.** The degree distribution does not take edge weights into account but treats all edges as equivalent. The single node with degree 24 is the West Baray, the largest of Angkor's reservoirs. The high degree is due to many small nodes in the central district feeding into the reservoir.

**Table S1. List of symbols for control parameters accompanied by their purpose in the overall algorithm (role), brief description, and units.**

| Symbol | Role | Description | Units |
|---|---|---|---|
| $\gamma$ | Flood control parameter | Determines magnitude of flood | N.A. |
| $k$ | Flood model control parameter | Shape parameter determining distribution of $X_i$ | N.A. |
| $\alpha$ | Cascading failure model control parameter | Determines sensitivity to erosion | N.A. |
| $\beta$ | Cascading failure model control parameter | Determines sensitivity to sedimentation | N.A. |

**Table S2. List of symbols for noncontrol parameters, accompanied by their purpose in the overall algorithm (role), brief description, and units.**

| Symbol | Role | Description | Units |
|---|---|---|---|
| $w_i$ | Initialization | Weight of edge $i$ estimated from GIS data | N.A. |
| $f_{eq}$ | Initialization | Initial equilibrium flow from super-source | $m^3\ s^{-1}$ |
| $f_i^o$ | Initialization | Initial equilibrium flow through edge $i$ | $m^3\ s^{-1}$ |
| $v_o$ | Initialization | Initial (uniform) fluid velocity | $m^3\ s^{-1}$ |
| $c_i^o$ | Initialization | Initial flow capacity of edge $i$, $c_i^o = f_i^o / v_o$ | $m^2$ |
| $v_o^i$ | Initialization | Initial fluid velocity over edge $i$, $v_o^i = f_i^o / c_i^o$ | $m^3\ s^{-1}$ |
| $f_{tot}$ | Flood model | Flow from super source during flood, $f_{tot} = f_{eq} + \gamma f_{eq}$ | $m^3\ s^{-1}$ |
| $X_i$ | Flood model | Stochastic perturbation to flow on edge $i$ | $m^3\ s^{-1}$ |
| $\theta_i$ | Flood model | Scale parameter determining distribution of $X_i$ , $\theta = f_i^o \gamma k^{-1}$ , $X_i \sim \Gamma(\theta, k)$ | $m^3\ s^{-1}$ |
| $f_i(t)$ | Cascading failure model | Flow over edge $i$ at time (iteration) $t$ , $f_i(0) = f_i^o + X_i$ | $m^3\ s^{-1}$ |
| $c_i(t)$ | Cascading failure model | Capacity of edge $i$ at iteration $t$ | $m^2$ |
| $v_i(t)$ | Cascading failure model | Fluid velocity on edge $i$ at iteration $t$ | $m^3\ s^{-1}$ |
| $v_{max}$ | Cascading failure model | Fluid velocity threshold beyond which erosion occurs, $v_{max} = v_o \alpha^{-1}$ | $m^3\ s^{-1}$ |
| $v_{min}$ | Cascading failure model | Fluid velocity threshold beyond which sedimentation occurs, $v_{min} = \beta v_o$ | $m^3\ s^{-1}$ |